Natural Hazards (2021) 108:3021–3043
https://doi.org/10.1007/s11069-021-04811-9

ORIGINAL PAPER

Characterization of a landslide-triggered debris flow at a rainforest-covered mountain region in Brazil

Victor Carvalho Cabral[1,2] · Fábio Augusto Gomes Vieira Reis[1] · Fernando Mazo D'Affonseca[2] · Ana Lucía[2] · Claudia Vanessa dos Santos Corrêa[1] · Vinicius Veloso[1] · Marcelo Fischer Gramani[3] · Agostinho Tadashi Ogura[3] · Andrea Fregolente Lazaretti[4] · Felipe Vemado[5] · Augusto José Pereira Filho[5] · Claudia Cristina dos Santos[6] · Eymar Silva Sampaio Lopes[6] · Lis Maria Reoni Rabaco[7] · Lucilia do Carmo Giordano[1] · Christiane Zarfl[2]

Received: 29 December 2020 / Accepted: 19 May 2021 / Published online: 30 May 2021

Abstract
Debris flows represent great hazard to humans due to their high destructive power. Understanding their hydrogeomorphic dynamics is fundamental in hazard assessment studies, especially in subtropical and tropical regions where debris flows have scarcely been studied when compared to other mass-wasting processes. Thus, this study aims at systematically analyzing the meteorological and geomorphological factors that characterize a landslide-triggered debris flow at the Pedra Branca catchment (Serra do Mar, Brazil), to quantify the debris flow's magnitude, peak discharge and velocity. A magnitude comparison with empirical equations (Italian Alps, Taiwan, Serra do Mar) is also conducted. The meteorological analysis is based on satellite data and rain gauge measurements, while the geomorphological characterization is based on terrestrial and aerial investigations, with high spatial resolution. The results indicate that it was a large-sized stony debris flow, with a total magnitude of 120,195 m^3, a peak discharge of 2146.7 $m^3\ s^{-1}$ and a peak velocity of 26.5 m s^{-1}. The debris flow was triggered by a 188-mm rainfall in 3 h (maximum intensity of 128 mm h^{-1}), with an estimated return period of 15 to 20 years, which, combined with the intense accumulation of on-channel debris (ca. 37,000 m^3), indicates that new high-magnitude debris flows in the catchment and the region are likely to occur within the next two decades. The knowledge of the potential frequency and magnitude (*F–M*) can support the creation of *F–M* relationships for Serra do Mar, a prerequisite for reliable hazard management and monitoring programs.

Keywords Shallow landslides · Magnitude · Serra do Mar · Forensic geomorphological analysis · Mass movements · Bedrock rivers

✉ Victor Carvalho Cabral
victor.carvalho@unesp.br

Extended author information available on the last page of the article

1 Introduction

Debris flows pose great threat to human life and infrastructure, especially in mountain regions, due to their sudden occurrence, high mobility, volume, impact energy and large run-out distance (Iverson 2000; Begueria et al. 2009; Luna et al. 2012). These phenomena occur when a mixture of earth material, water and air very rapidly surges down steep drainage paths (Varnes 1978; Takahashi 2006; Hungr et al. 2014) and their primary triggering factor is high-intensity rainfall (Milne et al. 2008). The increasing frequency of extreme rainfall events on a global scale (Beniston 2009; Giorgi et al. 2011; Borga et al. 2014; Westra et al. 2014) has been associated with an observed increase in the frequency and magnitude of debris-flow events (Stoffel and Huggel 2012; Winter and Shearer 2014; Borga et al. 2014), which, combined with landslides, were responsible for more than 32,000 casualties between 2004 and 2010 (Petley 2012; Borga et al. 2014).

An increase in the frequency of extreme precipitation events has also been observed for southern and southeastern Brazil (Teixeira and Satyamurti 2011), which could alter mass movement dynamics in the country. Over 4000 debris-flow-related fatalities were recorded in the last 100 years from 22 fatal events in Brazil (Kobiyama et al. 2015), 95% of which concentrated at the Serra do Mar, a mountain range that extends for about 1500 km in the southern and southeastern coast (Vieira and Gramani 2015). Despite their highly destructive potential, debris flows are still poorly studied when compared to other mass-wasting processes in Brazil, mainly due to insufficient monitoring (Borga et al. 2014; Kobiyama et al. 2015; Gregoretti et al. 2018).

Direct field investigations are essential for understanding the hydrogeomorphic dynamics of a catchment during debris flows (Gaume and Borga 2008; Borga et al. 2014; Lucía et al. 2018). They also provide a sound knowledge of the magnitude of a debris-flow event (i.e., the total volume of transported debris), which is a prerequisite for understanding and quantifying associated hazards (Jakob 2005a). The irregular occurrence of debris flows, however, and their development in terrains of difficult, often dangerous, accessibility pose a challenge to detailed pre- and post-event field studies (Kean et al. 2013; Gregoretti et al. 2018; Destro et al. 2018).

Magnitude estimations are more commonly carried out by statistical and empirical methods (e.g., Takahashi 1992; Bianco and Franzi 2000; Massad 2002; Takahashi 2006; Kanji et al. 2007; Chang et al. 2011) or by post-event (forensic) geomorphological investigation of the debris-flow route in a catchment (e.g., Marchi and D'Agostino 2004; Liu et al. 2009; Gregoretti et al. 2018). Geomorphology-based estimations are considered one of the most accurate since they are based on direct field evidences (Liu et al. 2009; Gregoretti et al. 2018) and do not necessarily require information about previous events (Marchi and D'Agostino 2004), which can be rare in some mountain regions.

Due to the high costs and difficulties involved using direct field investigations, empirical equations have been developed to estimate magnitude, as a result of extensive debris-flow documentation in highly prone regions, such as the European Alps, west coast of North America, Japan and Taiwan (e.g., Kronfellner-Krauss 1985; Takei 1984; Takahashi 1991; Rickenmann and Zimmermann 1993; Marchi and D'Agostino 2004; Chang et al. 2011). Empirical equations and semiempirical equations, however, are mainly site-specific (Rickenmann 1999; Gregoretti et al. 2018) and can potentially be inadequate in areas with different geological-geomorphological settings.

By estimating the magnitude, important kinematic parameters such as peak discharge and flow velocity can also be obtained (Rickenmann 1999; Pak and Lee 2008; Santi et al.

2008; Reid et al. 2016), which are crucial in the proper design of retention structures (Kanji et al 2007; Santi 2014; Gregoretti et al. 2018). Peak discharge and velocity are directly related to the entrainment potential of debris flows, which can significantly increase the magnitude, in some cases by an order of magnitude, and the overall hazard of the process (Milne 2008; Santi et al. 2008; Berger et al. 2011; de Hass and Densmore 2019).

Debris-flow magnitude estimations based on forensic geomorphological characterizations are scarce in mountain regions (Stoffel 2010), being often focused on flash-flood events (e.g., Gaume and Borga 2008; Borga et al. 2014; Surian et al. 2016; Steeb et al. 2017; Lucía et al. 2018) or are mostly concentrated on alpine catchments with extensive documented history of debris-flow events (e.g., Marchi and D'Agostino 2004; Tang et al. 2011; Gregoretti et al. 2018). For Serra do Mar in Brazil, which is a region typical for rainstorms that often trigger mass movements (Vieira and Gramani 2015), such studies are non-existent.

In this study, we characterize a landslide-triggered debris flow that occurred on February 11, 2017, at the Pedra Branca catchment in the Serra do Mar mountain range. A forensic geomorphological analysis with an unprecedented spatial resolution is conducted to characterize the source area, transport path and deposits of the debris flow and to estimate the debris flow's magnitude, peak discharge and flow velocity. A forensic meteorological characterization is also performed to analyze the precipitation pattern of the debris-flow event, based on satellite data and rain gauge measurements.

Furthermore, a comparison between the geomorphology-based estimation with magnitudes calculated using empirical equations from the literature is conducted to assess their applicability to the study area, which can support further debris-flow susceptibility studies for Serra Mar. The equations are chosen due to their simplicity in input parameters (Italian alps—Marchi and D'Agostino 2004; Marchi et al. 2019), their consideration of rainfall and landslides volume in calculations (Taiwan—Chang et al. 2011) and the similar geological–geomorphological context (Serra do Mar—Kanji et al. 2007).

2 Study area

The Pedra Branca catchment (Fig. 1) is characterized by a great difference in altitude when compared to the surrounding region, with elevations that range from 90 to 1100 m a.s.l (above sea level). The 3.43 km^2 catchment exhibits moderate drainage density (3 km km^{-2}) and a relief ratio (0.35) and Melton number (0.6) that indicate the tendency to initiate debris flows and debris floods (Wilford et al. 2004) (Table 1).

In the region, rainfall is well distributed year-round, averaging 2500 mm annually and reaching up to 3500 mm in some years (Maack 2002; Mocochinski and Scheer 2014). The Proterozoic monzogranite that comprises the bedrock of Pedra Branca's headwaters is one of the most weathering-resistant rock types in Serra do Mar (Vieira and Gramani 2015), generating shallow residual soil (up to 2 m deep) and steep slopes that stand out in the landform (Fig. 2b). The catchment is covered by the Atlantic Forest biome, a tall, broadleaf rainforest, considered the second largest tropical forest of the American continent (Tabarelli et al. 2005).

The February 2017 debris flow was initiated by shallow landslides in the headwaters' region. Three landslides were identified as the triggers of the event (highlighted in red in Fig. 2), from a total of 17 landslide scars mapped. For the sake of simplicity, merged

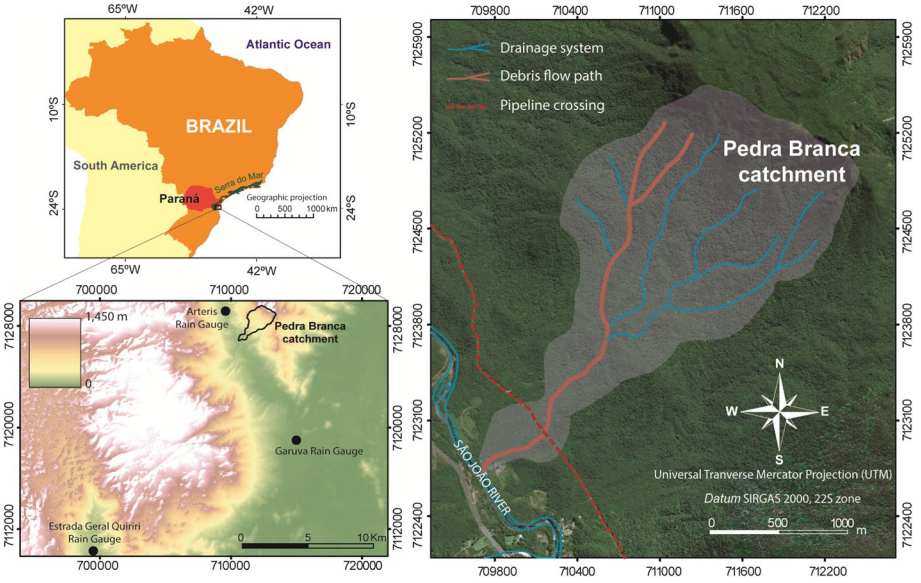

Fig. 1 Pedra Branca catchment (right) in the municipality of Guaratuba, State of Paraná, Brazil. At the top left, the extension of the Serra do Mar mountain range. At the bottom left, the digital terrain model (DTM) for the broader region of the catchment with the location of the three nearest rain gauges

Table 1 Pedra Branca's physiographic features

Parameter	Formulae	Value	Unit
Watershed area	–	3.43	km^2
Maximum elevation	–	1100	m a.s.l
Elevation at the outlet region	–	90	m a.s.l
Average watershed slope	–	16.8	Degrees
Channel length	–	2900	m
Slope at the initiation area	–	67/34	Percent/degrees
Slope at the outlet region	–	7/4	Percent/degrees
Average channel slope	–	18/10	Percent/degrees
Drainage density	L_t/A	3	$km\ km^{-2}$
Relief ratio	H_t/L_h	0.35	$km\ km^{-1}$
Melton ratio[a]	$H_t/A^{-1/2}$	0.6	–

H_t is maximum amplitude, L_t is length of channels, A is watershed area, L_h is watershed length

[a]Melton ratio is a morphometric parameter used to differentiate flood and debris-flow-prone catchments. Debris-flow-prone catchments generally have > 0.6 (Wilford et al. 2004)

scars were counted as one single scar. The debris flow affected oil pipelines that cross the catchment (buried at a 1 m depth) and destroyed a small bridge and a farm located at the outlet region. An interview with one of the affected farmers describing the event is available as supplementary data. No casualties were reported.

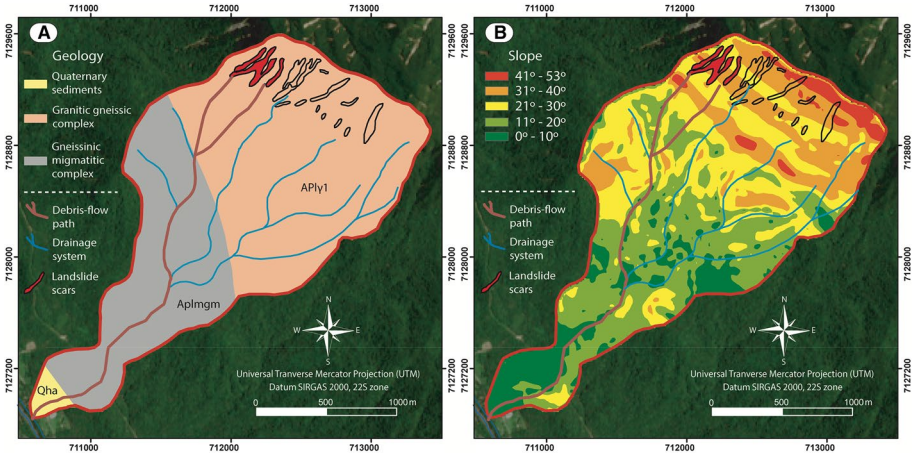

Fig. 2 **a** Geological map of the Pedra Branca catchment based on the 1:250,000 map (Folha Curitiba) made by the Geological Service of the State of Paraná (Mineropar). Qha—Quaternary fluvial sediments and alluvium. APlγ1—Archean/Lower Proterozoic monzogranites, porphyritic and equigranular. APlmgm—Archean/Lower Proterozoic ophthalmic migmatites, with biotite gneiss paleosome. **b** Slope map of the catchment based on a topographic map at a scale of 1:25,000. Landslide scars that triggered the debris flow are highlighted in red

3 Materials and methods

3.1 Forensic meteorological analysis

The rainfall analysis combined satellite and rain gauge data. The Geostationary Operational Environmental Satellite (GOES13) was used to characterize the start time and duration of the precipitation event, while intensity was retrieved from rain gauge measurements. The nearest rain gauge, located 1 km away from Pedra Branca, is controlled by the private company Arteris—Litoral Sul, which provided hourly rainfall measurements for the month of February 2017 (Arteris Rain Gauge, Fig. 1). The other two rain gauges are part of the Brazilian rain gauge network, and their measurements are freely available, provided by CEMADEN (Centro Nacional de Monitoramento e Alerta de Desastres Naturais 2020) and ANA (Agência Nacional de Águas 2020). The 'Garuva' rain gauge is located approximately 10 km southeastward of Pedra Branca catchment, while 'Estrada Geral Quiriri' is located 30 km southward (Fig. 1).

3.2 Forensic geomorphological analysis

Terrestrial and aerial investigation was carried out to characterize the physiography of the catchment after the debris flow. Field campaigns were conducted one and six months after the event (March and August 2017) to characterize post-event geomorphological features and to acquire high-resolution aerial photographs of the debris-flow path using an unmanned aerial vehicle (UAV).

Field observations were determinant in the identification of the sediment budget of the channel, aiding the assessment of the event's characteristics (a channelized, stony debris

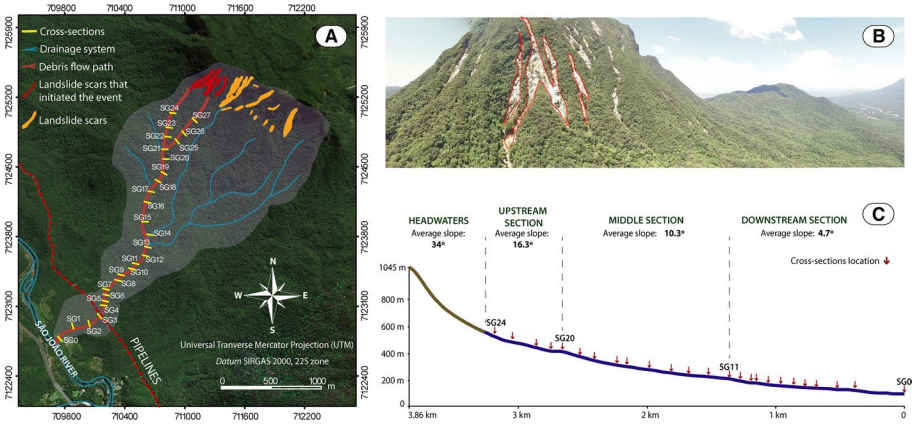

Fig. 3 **a** Location of the 28 cross-sections made along the debris-flow path. **b** Overview of the headwaters' region of the catchment, highlighting the three landslide scars that initiated the debris flow. **c** Longitudinal profile of Pedra Branca catchment with the tentative location of the cross sections. Channel in blue and slopes in brown

flow) and the movement dynamics in the catchment. On-channel deposits were assessed using cross sections made along the Pedra Branca riverbed (available as supplementary material), which also depicted post-event channel width. Peak flow marks were documented, as well as estimated erosion depths, based on erosion marks and bedrock exposures. The measurements were made with the help of range finders, measuring tapes, rods and levels. A total of 28 cross sections were surveyed at approximately every 120 m along the debris-flow route (Fig. 3).

The orthorectified aerial photographs further allowed the identification and delimitation of debris accumulation areas along the channel, as well as the delimitation of entrainment areas along the riverbed and lateral slopes and banks. Sediment sources located at the headwaters (i.e., landslides) were identified and delimitated using non-orthorectified aerial photographs retrieved from the UAV survey. The drone DJI Phantom 3 was employed in the UAV survey, equipped with a camera with focal length of 3.61 mm and ground sampling distance (GSD) of 8.654 cm/pixel. Twenty-three (23) targets were used for georeferencing the orthophotos, which were processed with the software PIX4D. The UAV overflight was done between August 28 and 30, 2017, in constant height of 200 m. The targets' coordinates were measured using a differential GPS (generating point presenting accuracy of 10 cm).

3.3 Magnitude estimation

The debris-flow magnitude was estimated based on the parameters obtained from the forensic analysis. The total volume (V_t) of the debris flow was calculated according to Jakob (2005a), being a mass balance of the landslides volume (V_i) that initiated the event, the volume of material entrained (V_e) by the flow and the volume deposited (V_d) along its path:

$$V_t = V_i + V_e - V_d. \quad (1)$$

V_i was estimated using the equation:

$$V_{\mathrm{i}} = A_i * e \tag{2}$$

where A_i is the landslides area (m^2) and e the average depth of the landslides (1 m, estimated using the aerial photographs from the UAV survey), assuming that the totality of the material reached the channel.

The calculation of on-channel debris volume (V_{d}) is based on the areas of accumulation (A_{d}), delimitated with orthophotos, and on the average depth of the deposits (e_{d}) observed and depicted at the 28 cross sections. In this study, Large Wood (logs with ≥ 10 cm in diameter and ≥ 1 m in length) is not individualized from other debris-types when estimating magnitude.

$$V_{\mathrm{d}} = \sum (A_{\mathrm{d}} * e_{\mathrm{d}}). \tag{3}$$

The entrained volume (V_{e}) is based on the identification of erosional areas (A_{e}) and on the erosion depth (e_{e}) documented during field campaigns:

$$V_{\mathrm{e}} = \sum (A_{\mathrm{e}} * e_{\mathrm{e}}). \tag{4}$$

At the intervals between cross sections, average depth values of erosion and deposition were applied.

Peak discharge (Q_{max}) is calculated based on the equation described in Jakob (2005a) and Chen et al. (2007):

$$Q_{\mathrm{max}} = A_{\mathrm{max}} * v_f \tag{5}$$

where A_{max} is the maximum cross-sectional area of the channel and v_f is the mean cross-sectional velocity during the time that the peak flow occurs. A_{max} is obtained from the 28 cross sections, and v_f is estimated according to the Manning–Strickler Eq. (6), traditional fluid-mechanics equation for Newtonian turbulent flows that considers the physiography of the river channel and can be suited to debris flows (Rickenmann 1999):

$$v_f = \left(\frac{1}{n}\right) * H^{\frac{2}{3}} * S^{\frac{1}{2}}. \tag{6}$$

Here, H is the maximum flow height (m) measured in the field, S is the channel bed slope, and n is the Manning coefficient (0.07 $m^{1/2}$ s^{-1}) for bedrock rivers in mountain regions (Arcement and Schneider 1989; Takahashi 2006).

Furthermore, empirical equations from the literature are also employed in magnitude estimation. Based on sediment volume data collected in the Eastern Italian Alps, Marchi and D'Agostino (2004) suggest that the magnitude of a debris-flow event can be estimated according to the geomorphometric characteristics of a catchment, as per the equation:

$$V = 65,000 * A^{1.35} * S^{1.7} \tag{7}$$

where A is the catchment area (km^2) and S the average channel slope (%). More recently, Marchi et al. (2019) updated Eq. 7 using a larger dataset and considering the severity of an event when estimating magnitude:

$$V = \mathrm{K} * A^{\gamma}. \tag{8}$$

Here, K (intercept) and γ (slope) represent the scaling parameters. Considering a moderate to large magnitude to the February 2017 event, the scaling parameters chosen to be

assessed in this study are related, respectively, to the 50th, 98th and 99th percentile of the dataset presented in Marchi et al. (2019):

$$V = (2620 \pm 60) * A^{0.67 \pm 0.02} \tag{9}$$

$$V = (52000 \pm 4000) * A^{0.94 \pm 0.04} \tag{10}$$

$$V = (77000 \pm 7000) * A^{1.01 \pm 0.06}. \tag{11}$$

Chang et al. (2011), based on 59 debris-flow-prone catchments in Taiwan, found that the magnitude can be estimated by the equation:

$$V = 0.023A_{\mathrm{w}} + 0.064A_{\mathrm{l}} + 13264.6\mathrm{GI} - 1399.2D + 38.47C_{\mathrm{R}}. \tag{12}$$

Here, A_{w} is the watershed area (m^2), A_{l} the landslide area (m^2), GI the geological index (dimensionless) based on Marchi and D'Agostino (2004), D the rainfall duration (h) and C_{R} the rainfall intensity (mm). Due to the uniform geology of Pedra Branca, comprised of crystalline rocks, the GI adopted is 0.5 (Marchi and D'Agostino 2004; Chang et al. 2011).

The equation presented in Kanji et al. (2007) considers that the magnitude (V) of a debris flow, assuming that these phenomena have a concentration of solids that vary from 40 to 80% (George and Iverson 2011), is a function of the concentration of solids per unit volume (c, Eq. 14) from Takahashi (1991), the catchment area (A, km^2) and the rainfall intensity one hour preceding the debris flow (I_1, mm):

$$V = \frac{1000 \cdot c}{1 - c} \cdot A \cdot I_1 \tag{13}$$

$$c = \rho_0 * \frac{tg\theta}{(\delta - \rho_0) \cdot (tg\phi - tg\theta)} \tag{14}$$

where θ is the average slope of the channel, ρ_0 is the specific weight of the slurry, δ is the granular material specific weight and ϕ is the internal friction angle of the sediments. For simplicity, and since the physical parameters of the studied debris flow were not determined, $c = 60\%$ is adopted, as suggested by Takahashi (1991, 2006) for stony debris flows.

For further magnitude studies and empirical equations, we refer to Hungr et al. (1984), Rickenmann (1999), Takahashi (1992, 20061991), Rickenmann and Koschini (2010) and Reid et al. (2016), among others.

4 Results

4.1 Forensic meteorological characterization

According to the testimonies of local farmers, the landslides that triggered the debris flow initiated between 2300 and 0000 UTC (20:00 and 21:00 local time—LT) on February 11. The landslides were triggered by an accumulated rainfall of 188 mm in 3 h, with maximum registered intensity of 128 mm h^{-1}, according to the nearest rain gauge data (Arteris—Fig. 4). The rainfall ended at approximately 0700 UTC (4:00 LT) on February 12, assuming that a precipitation event ends when in six consecutive hours the accumulated rainfall

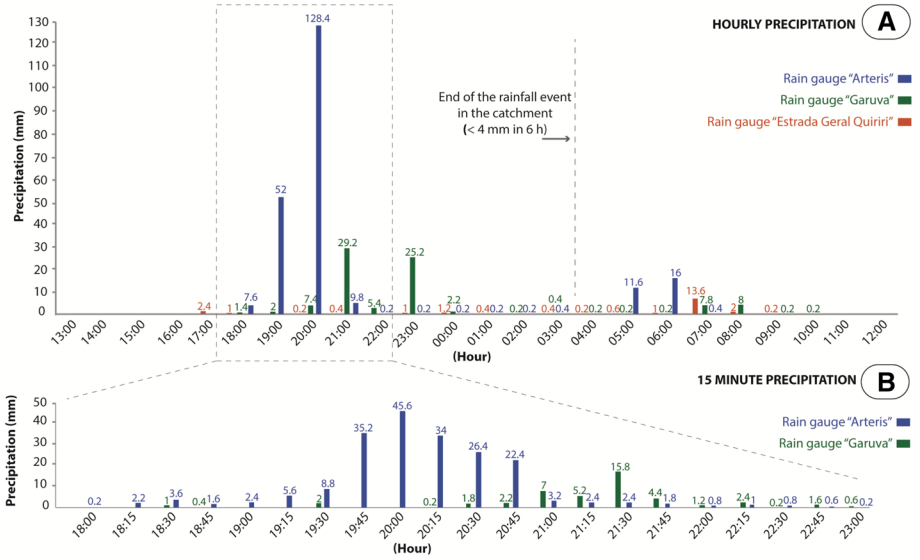

Fig. 4 **a** Hourly precipitation for February 11 and 12, 2017, according to the three nearest rain gauges. Rain gauge 'Arteris' is located 1 km from Pedra Branca catchment, while 'Garuva' and 'Estrada Geral Quiriri' are located at approximately 10 km and 30 km away, respectively. **b** Precipitation recorded every 15 min by the rain gauges 'Arteris' and 'Garuva' between 18:00 LT (2100 UTC) and 23:00 (0200 UTC)

is less than 4 mm (Chang et al. 2011). As the recorded antecedent rainfall for the preceding 10 days is estimated at around 88 mm, 23 mm of which (26%) in the last 48 h before the event, soil water content was already significant.

Precipitation recorded by the rain gauges integrated to the Brazilian pluviometer network (Fig. 4) is notably lower than what the nearest rain gauge documented, suggesting that the extreme rainfall rates were mainly concentrated near the hillslopes of Pedra Branca as a result of orographic effect. The rain gauge 'Garuva' recorded 72.8 mm in 12 h, with a maximum intensity of 29.2 mm h^{-1}, while the rain gauge 'Estrada Geral Quiriri' barely recorded the event. Considering the difference in precipitation rates and the lag-time of 1 h between the rain gauges 'Arteris' and 'Garuva,' it is suggested that the event developed from north to south and lost intensity during its trajectory.

The data from the GOES13 satellite indicate that the rainfall in the broader region of Pedra Branca initiated at around 1800UTC (15:00 LT) on February 11 and ended at around 0700UTC (04:00 LT), as also shown by rain gauge data. Cloud tops reached 13-km altitude over the catchment, with high rainfall rates for about 4 h, continuously. The return period for a rainfall with such intensity is estimated between 15 and 20 years, based on heavy-rainfall equations for the region (Back et al. 2011; Pereira Filho et al. 2018).

4.2 Forensic geomorphological analysis

The three shallow landslides that triggered the debris flow have their upgradient portions in moderate slopes (38–61%, or 21° to 31°), while those originated in steeper slopes (> 61%, or > 31°) did not initiate an event in the other tributaries, probably due to thinner residual soils and colluvium (i.e., less material to generate a debris flow).

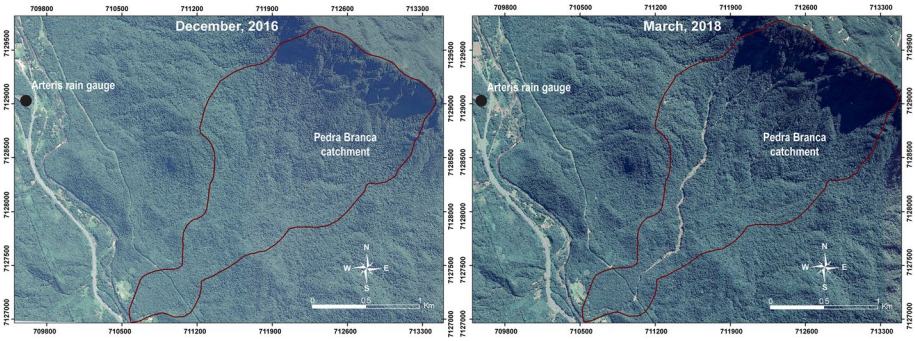

Fig. 5 Before (left) and after (right) the debris-flow event at the Pedra Branca catchment. Aerial photographs from December 2016 and March 2018, from Google time-lapse. The location of the nearest rain gauge (Arteris) is indicated (Highway BR-376, km 676 + 800 m)

The mobilized materials by the three landslides are mainly residual soil and large wood, which suggest loss of suction as the initiation mechanism at the study area. The debris flow was initiated by first-time movements in the hillslopes (mapped in Fig. 3), but also carried material (colluvium) from previous landslides, accumulated at the upper portion of the channel.

The channelization of the material mobilized by the landslides contributed to a magnification of the erosional process, with a pronounced entrainment and scour of debris at the upstream section of the channel. Erosion of the channel bed, lateral slopes and banks by the debris flow progressively decreased toward the outlet region, ranging from an average depth of 3 m at the upstream section to 0.3 m downstream. In bedrock exposed areas, erosion depth was assumed as 0 and the average depth between two sections was used in entrainment calculation, since no information about previous on-channel deposits or channel morphology is available. Bedrock exposed areas are mainly located in steep portions of the channel near the initiation area and in knickpoints (Fig. 5).

On-channel debris at the upstream section (between SG20 and SG24/SG27) consists mainly of large monzogranite boulders (2 to 5 m in diameter), deposited at the perimeter of the flow route or exhumed from colluvial deposits of the lateral slopes (Fig. 6a). On-channel debris accumulation becomes more frequent toward the catchment's outlet (Fig. 7c), with the largest volume of debris deposited at the middle portion of the channel (between SG11 and SG19, Fig. 6b) where the average slope is 18.2% (10.3°), i.e., within the range of deposition angles for channelized debris flows (from 14 to 21%) (Iverson et al. 2011). Debris deposition also occurs at the downstream portion of the catchment (SG0 to SG10), although with smaller-sized boulders (< 2 m in diameter) and less voluminous deposits than at the middle portion (Fig. 6c). Recent on-channel debris deposits are easily identified from colluvial deposits due to the lack of pedogenetic evidences and the mixture of fresh wood and stony debris (Fig. 6d).

Large wood (LW) deposition and accumulation, differently from stony debris, are more frequent at the downstream section of the channel (SG11 to SG0). At this section, the influence of LW in the debris-flow evolution is prominent, with evidences of LW jams that were broken by the flow passage (Fig. 7a). Debris dams (i.e., areas with intense debris deposition, blocking partially the flow) are observed along the channel and are in their majority clast supported with woody debris (Fig. 7b), often exhibiting reversely graded patterns.

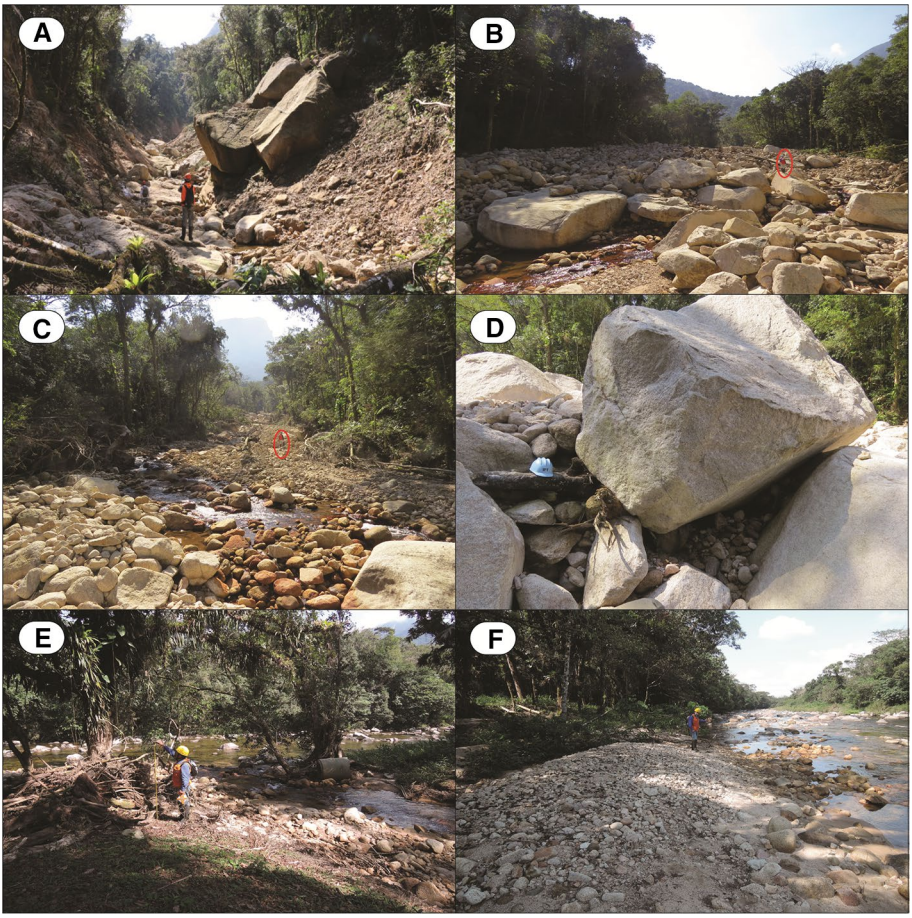

Fig. 6 **a** Pronounced erosion and scour of channel bed are observed at the upstream section (SG23)—1.8 m human profile for scaling. **b** Intense accumulation of debris at the middle section (SG13)—in detail, a 1.75 m human profile for scaling. **c** Accumulation of debris at the downstream section (SG6), with smaller-sized boulders than in the middle section—1.75 m human profile for scaling. **d** Reversely graded pattern observed in debris dams (SG5). **e** Debouchment of the Pedra Branca River into the São João River, where flow height reached up to 2 m. **f** São João River, which received sediments from the Pedra Branca debris flow (photograph from August 2017)

The occurrence of these dams indicates that the debris flow had multiple surges, which is confirmed by the affected farmers that report at least four surges.

The imbricated boulders along the channel's length and the intense debris accumulation along at the middle section of the channel suggest that the event started as a debris flow, evolving into a debris flood as channel slope decreased. At the outlet region, according to testimonies, the flow consisted mainly of muddy water (with sand, silt, clay) mixed with woody debris (Fig. 6e) and, minorly, by stony debris of up to 1 m. These characteristics indicate that in the final stages, the event exhibited characteristics of a flash flood.

The average post-debris-flow width of the channel is ca. 20 m, ten times the previous average width (ca. 2 m) reported by testimonies (Fig. 5). No prominent alluvial fan is formed, due to narrow valley and discharge to the larger São João River (Fig. 6e). At

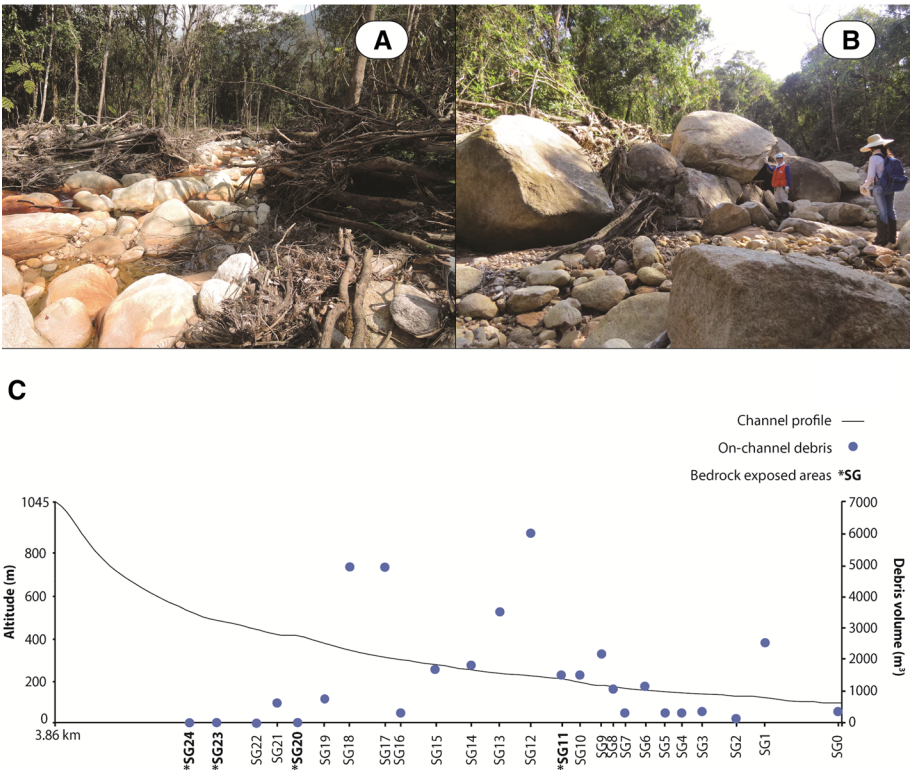

Fig. 7 **a** Large wood forming a jam that was later broken by the flow's passage (SG1). **b** Mixture of woody and stony debris and formation of debris dams (SG12)—1.75 m human profile for scaling. **c** Plot showing the Pedra Branca channel profile and the volume of deposited debris along the debris-flow route. Debris deposition is higher at the middle section of the channel (SG19 to SG11)

the São João River, large deposits of coarse sand or cobbles are accumulated near Pedra Branca outlet (Fig. 6f), as well as small- to medium-sized boulders (< 1.5 m in diameters) on the river channel.

The mapping of erosional and depositional areas along the Pedra Branca channel is shown in Fig. 8, based on the orthophotos. Even though debris deposition generally occurs in areas with gentler slope (Fig. 9a), a direct correlation between these two factors is not observed, with a very weak Spearman correlation coefficient (0.025) and regression line with very low R^2 (0.002) when their relationship is analyzed (Fig. 9c). Debris deposition, therefore, might be influenced by other factors, such as valley width, presence of obstacles and availability of coarse material itself, which can further be related to a less voluminous deposition in lower reaches of the channel with low slope than at intermediate reaches.

Erosion depth, on the other hand, shows a positive correlation with slope, being deeper near steeper portions of the channel (Fig. 9b). Excluding areas where bedrock exposure is observed, a correlation between slope and erosion depth shows a weak/moderate positive Spearman coefficient (0.39) and a regression line with a weak to moderate R^2 (0.3149) (Fig. 9d). Hence, erosion is moderately influenced by slope, which can further be associated with a higher momentum of the flow's passage in steeper reaches

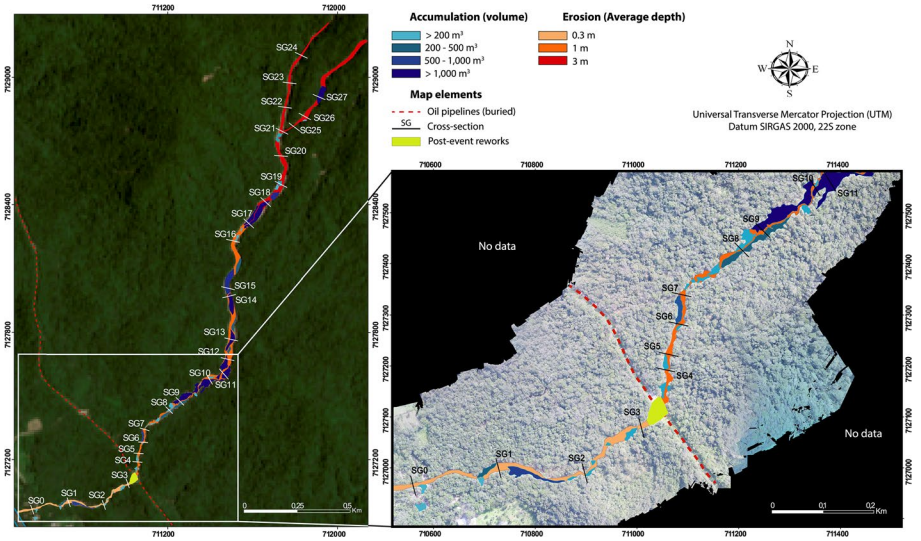

Fig. 8 Mapping of entrainment and deposition areas based on the orthophotos acquired using UAV. Areas in shades of blue represent debris accumulation areas, and areas in shades of red represent entrainment areas

of the channel. The exclusion of bedrock exposed reaches in the correlation is due to a different incision dynamic than at alluvial–colluvial reaches.

The distribution of maximum grain size (D_{90}) of debris along the debris-flow path shows that debris size decreased by approximately 80% along its trajectory (Fig. 9e). Sharp reductions in D_{90} along the channel are related to regions where intense debris deposition is observed. Flow heights are generally higher in regions downstream to knickpoints in the channel (between SG4 and SG5, SG10 and SG11, SG18 and 19), with the debris flow reaching a peak height of 7 m at the region of the cross-section SG9 (Fig. 9f). At the debouchment into the larger São João River, flow heights were up to 2 m (Fig. 9f). Flow height can be affected by areas with intense debris accumulation, which can partially block the flow and raise the flow level. To minimize the uncertainties related to forensic discharge estimations, we documented flow heights in areas that were not directly affected by the intense accumulation of stony and woody debris.

4.3 Magnitude estimation

The total volume of the debris flow (V_t) is estimated at approximately 120,195 m^3, based on the mapping of entrainment and deposition areas (Fig. 7) and on the landslides that initiated the event. Volume entrained by the flow (V_e) is estimated at 121,037 m^3, while the volume of debris deposited along the debris-flow path (V_d) accumulates to 36,688 m^3. The table with the measurements used in the calculation of entrained and deposited volumes is available as supplementary material.

The three landslides that initiated the event contributed with 35,846 m^3 of earth material. The largest landslide scar contributed with 22,497 m^3, while the other two contributed with 7573 m^3 and 5776 m^3, assuming an average depth of 1 m and that the totality of the

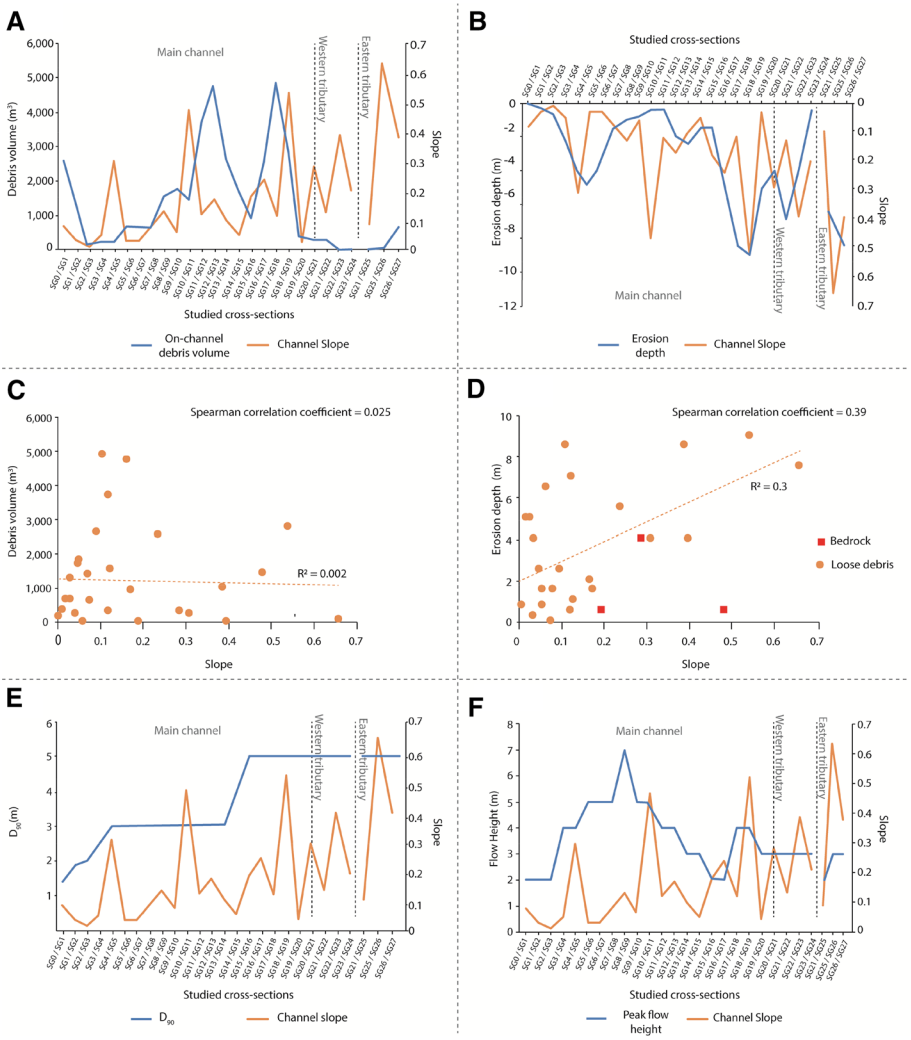

Fig. 9 a Distribution of on-channel debris volume along the debris-flow path in relation to channel slope. **b** Erosion depth distribution along the debris-flow path in relation to channel slope. **c** Scatterplot showing the relationship between on-channel debris volume and channel slope. **d** Scatterplot showing the relationship between erosion depth and channel slope. Bedrock and loose debris refer to the on-channel material post-event. **e** Maximum debris size (D_{90}) distribution along the debris-flow path in relation to channel slope (measured between every two cross-sections). **f** Peak flow height distribution in relation to channel slope

material reached the channel. Despite the uncertainties associated with erosion depth at the study area, due to the unknown channel morphology before the event, it is evident that entrainment significantly increased the total magnitude of the process, representing more than 75% of earth material input.

Moreover, subjectivity and human error might decrease accuracy and is challenging to be considered during calculations. Nonetheless, our estimations suggest that the February 2017 debris flow had a large magnitude, within the range of the size class 5 (10^5–10^6

Table 2 Magnitude of the February 2017 debris flow, estimated according to empirical equations and the forensic geomorphological characterization

Author	Magnitude
Marchi and D'Agostino (2004)	18,600 m^3
Marchi et al. (2019)—50th percentile	5983 ± 290 m^3
Marchi et al. (2019)—98th percentile	$165{,}645 \pm 22{,}000$ m^3
Marchi et al. (2019)—99th percentile	$267{,}385 \pm 46{,}000$ m^3
Kanji et al. (2007)	439,040 m^3
Chang et al. (2011)	90,851 m^3
This study	120,195 m^3

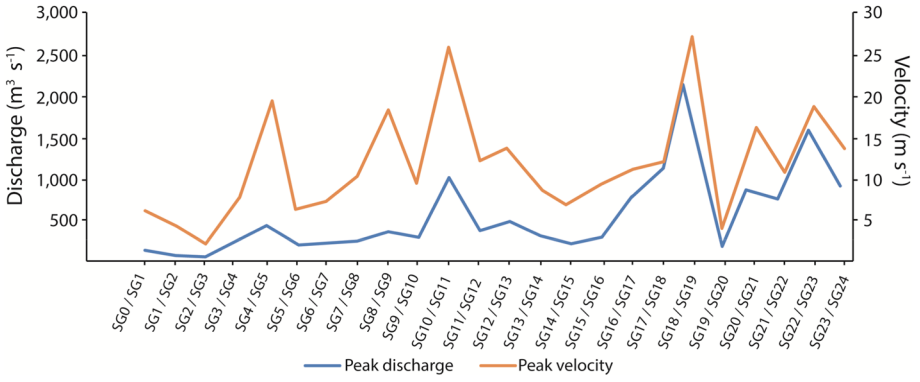

Fig. 10 Discharge and flow velocity pattern along the debris-flow path

m^3) proposed by Jakob (2005b). Size-class 5 debris flows can destroy parts of villages and infrastructures, destroy forest of up 2 km^2 and block creeks and rivers (Jakob 2005b).

Comparing our field-based magnitude estimates with the results using empirical equations (Table 2), the equation from Marchi et al. (2019) is the best-fit for the study area. While using the scaling parameters of the 50th and 99th percentile considerably underestimated (ca. 5983 m^3, 95% less than our estimates) and overestimated (ca. 267,385, 121% more) the magnitude, the 98th percentile resulted in an approximate magnitude (ca. 143,645 m^3, 18% more) when considering the lower error threshold.

The equation based on Taiwanese debris-flow cases, from Chang et al. (2011), also provided fairly good results, estimating the magnitude at ca. 91,000 m^3, which is 24% less than the value calculated based on in situ data. Marchi and D'Agostino (2004) equation performed similarly to the 50th percentile of the updated version of the equation presented in Marchi et al. (2019), also underestimating the magnitude (18,600 m^3, 84% less than our estimations). The equations shown in Kanji et al. (2007) highly overestimated the magnitude (439,040 m^3, 265% more than our estimations).

Highest discharge and velocity rates are observed between cross-sections SG18 and SG19 (2146.7 m^3 s^{-1} and 29.04 m s^{-1}, respectively), where channel slope is the steepest and cross-sectional area one of the largest. Discharge, in general, is higher at the immediate region downstream to the initiation area (SG24 to SG22 and SG27 to SG25) and at the confluency of the two tributaries (Between SG21 to SG17), progressively decreasing toward the outlet region (Fig. 10). Velocity rate patterns are similar to the discharge

(Fig. 10). The table with the measurements used in the discharge and velocity calculation is also available as supplementary material.

At the region of the oil pipelines (SG3 and SG4), discharge was approximately 228 $m^3\ s^{-1}$ and flow velocity 7.9 m s^{-1}, which can be associated with their preservation due to the relatively weaker and slower flow at that region. It is important to point out, however, that the concurrence of debris flows and debris/flash floods might increase the uncertainty over peak discharge estimations, due to an alteration of the channel cross-section stability with the passage of large sediment volume (Amponsah et al. 2016; Destro et al. 2018).

5 Discussion

The available rainfall data suggest that the high-intensity precipitation was sharply localized over Pedra Branca hillslopes and had a short duration. Rainfall estimations, however, might be underestimated due to the location of the rain gauges at the valley and not at the hillslopes, where landslides initiate. The estimated return period of the high-intensity rainfall in the region, combined with the large amount of mobilizable on-channel debris at Pedra Branca (ca. 37,000 m^3), suggests that new high-magnitude debris flows can potentially occur in the region in the near future (next one or two decades).

The debris flow was triggered by three large landslides, which initiating mechanism is interpreted as loss of suction due to a local rise in the water table by rainfall infiltration. Loss of suction is a common initiation factor at crystalline areas at the Serra do Mar mountain range (Wolle and Hachich 1989; Lacerda 2007) and is attributed to saturation levels reaching depths below the root zone of the soil. Soil saturation level at the hillslope region was already significant due to the antecedent rainfall (23 mm in the previous 48 h), and the sudden rise in the water table, as a result of the high rainfall rates (128 mm h^{-1}), led to slope failure.

Debris flows at Serra do Mar are generally triggered by high precipitation rates accumulated in 72 h, with peak rainfall of > 60 mm h^{-1} (Kanji et al. 1997). The lack of past debris-flow data for the Pedra Branca catchment and the surrounding region is a challenge for the creation of a site-specific rainfall thresholds that could support the development of an early warning system (EWS) in the region. Consequently, thresholds developed for different parts of Serra do Mar could preliminarily be adapted and updated for Pedra Branca, such as the one from Kanji et al. (1997). A constant update of these rainfall thresholds is necessary, especially considering the projected increase in the frequency of extreme rainfall events for the south and southeast of Brazil (Marengo et al. 2021) and that these equations were created more than 20 years ago.

Debris-flow initiation is not controlled solely by rainfall, as it also depends on debris supply and recharge rate, which influences the magnitude and the frequency of new events in a catchment. The debris flow in the Pedra Branca catchment had a magnitude of approximately 120,000 m^3, thus a large debris flow. According to Jakob (2005b), such magnitude for a boulder-rich debris flows is atypical, although the statement could be biased due to the general lack of magnitude studies worldwide, especially in mountain areas where debris-flow studies are still incipient. At Serra do Mar, based on the few available magnitude estimates (e.g., Kanji et al. 2007; Kobiyama et al. 2015), 10^5 m^3 debris flows are what is usually reported, probably also due to a bias toward reporting and characterizing only larger events (such as the present study) and the lack of studies aiming at specifically estimating debris-flow magnitude.

The most suited empirical equation for our study area was the one based on the 98th percentile of the cases analyzed by Marchi et al. (2019) in the Italian alps, indicating that a debris flow with the same magnitude as Pedra Branca has a ca. 2% probability to occur in that region. This could also suggest that at Serra do Mar large debris flows occur less often than smaller ones that tend to go unreported, but such statement is challenging considering the large dataset necessary to establish magnitude-frequency relationships and the differences in geological/geomorphological settings that affect debris-flow dynamics. More magnitude studies at Serra do Mar are recommended and necessary.

We suggest, therefore, that the equations from Marchi et al. (2019) should be tested in future events or in back-analysis studies in Brazil, to attest further its efficacy in representing debris-flow magnitudes in different mountainous areas. Even though the equation shown in Kanji et al. (2007) was created for a catchment at Serra do Mar (based on the 1994 debris flow at Rio das Pedras catchment, in Cubatão), it highly overestimated the magnitude of the Pedra Branca debris flow. This overestimation can be related to the equation's heavy reliance on the physical parameters of the debris flow, which was not tested in our study.

The equation by Marchi et al. (2019) introduces scaling parameters that amplifies the application of the equation when compared to the one presented in Marchi and D'Agostino (2004), which are adjusted according to different debris-flow scenarios and, consequently, can be applied to a wider variety of regions. The simple input parameters are another advantage, which favors it application on mountain regions where few information is available. Moreover, the equation from Chang et al. (2011) also provided approximate results compared to our estimates. While it underestimated the event (24% less than the forensic-based magnitude), the consideration of different parameters that influence the dynamics of a landslide-triggered debris flows (e.g., geology, rainfall, landslide area) can potentially be adequate for Serra do Mar, when a landslide inventory and rainfall data are available.

Forensic geomorphological analyses are fundamental for an accurate depiction of sediment mobilization in a catchment, supporting magnitude estimations and countermeasures dimensioning. Studies that characterize the magnitude of recent debris-flow events are key to support regional-scale studies, since they describe how a debris flow develops in a catchment, which characteristics are potential driving factors and quantify the hazard that similar catchments might be susceptible to.

The February 2017 event at the Pedra Branca catchment started as a debris flow at the upper portions of the catchment and, as channel slope decreased, it evolved into a debris flood and, at later stages, a flash flood as it progressed toward the outlet region. This evolution can be attributed to the progressive deposition of debris (especially large rock boulders) along the flow route, especially at the middle portion of the channel. The progressive decrease in discharge and flow velocity can also be attributed to the deposition of material along the channel, a direct result of gentler channel slope from the middle section on and the long length of the channel (2900 m), decreasing the flow momentum.

Flow momentum decrease is also associated with the entrainment potential of the debris flow, with a progressive reduction in erosion depth toward the debouchment area. Even though the estimation of eroded material is affected by larger uncertainties than the landslides and on-channel debris volume, the debris flow's sediment yield came mostly from the entrainment of material from channel bed and lateral banks, which is a common characteristic of large debris flows worldwide (e.g., Marchi et al. 2009; Gabet and Sternberg 2008; Bennet et al. 2013; Shen et al. 2020).

Despite the subjectivities and uncertainties related to the forensic-based estimation, it is the most accurate way to describe the hydrodynamic evolution of a debris flow in a channel

and is the base for simulation of debris flows using physically based models. It is also an important pathway for the establishment of *F–M* relationships, which, so far, are limited to a few selected regions in the world due to the long period of data required to construct meaningful relationships (Stoffel 2010; Huggel et al. 2012). The establishment of magnitude and frequency of debris-flow events is fundamental for accurate risk management.

Several other recent, deadly, debris flows have occurred at Serra do Mar that could have been mitigated if *F–M* studies and EWS were available, such as at Itaoca (State of São Paulo) in January 2014[1] and in the Teresópolis region[2] (State of Rio de Janeiro) in January 2011. These examples highlight the importance of sediment mobilization analysis in a catchment as well as the need for magnitude studies to quantify the potential damages that could result from debris-flow events and the frequency at which debris flows are expected to occur at Serra do Mar.

Studies on debris-flow frequency are recommended and necessary. Cosmogenic, optically stimulated luminescence (OSL) and radiocarbon dating of colluvial deposits are techniques that can be applied in frequency estimation of mass-wasting events in tropical and subtropical regions (Lang et al. 1999; Pánek 2014). Radiocarbon dating, due to lower costs and simpler sampling when compared to the other dating techniques (Pánek 2014), should be attempted in future at the Pedra Branca catchment, as well in high-hazard catchments at Serra do Mar. The large amount of mobilized LW and organic material by debris flows in the region provides reliable results (Lang et al. 1999). LW can contribute to increase debris-flow hazard (Lucía et al. 2015; Rickenmann 2016), and therefore, studies that consider LW mobilization in the densely forested catchments of Serra do Mar are encouraged.

6 Conclusion

This study characterized a debris flow that occurred at Serra do Mar in February 2017. The event was triggered by a 188-mm rainfall in 3 h (128 mm h^{-1} maximum intensity), with a return period of 15 to 20 years. The debris flow had a total magnitude of 120,195 m^3, with peak discharge of 2146.7 m^3 s^{-1} and peak velocity of 26.5 m s^{-1}. It was, therefore, a large magnitude stony debris flow triggered by a moderate return period precipitation. The debris flow dammed parts of the Pedra Branca channel, incisively eroded parts of the forest along its path and damaged infrastructures.

The documentation of recent debris-flow events, with magnitude and hydrogeomorphic dynamics characterization, is extremely critical for Serra do Mar, where debris-flow studies are still scarce. Magnitude studies for a catchment are important, since they are a pathway for the development of frequency–magnitude relationships that can support accurate hazard assessments and reliable monitoring programs. Moreover, the mapping of debris-flow-prone catchments throughout Serra do Mar is necessary to identify those that represent greater hazard and to prioritize the implementation of monitoring programs and EWSs.

Supplementary Information The online version contains supplementary material available at https://doi.org/10.1007/s11069-021-04811-9.

[1] Triggered by an accumulated rainfall of 210 mm in two hours, destroying houses and public infrastructures. 25 casualties were reported (Gramani and Martins 2016).

[2] Considered the 8th worst landslide event in world history by the United Nations (Rosi et al. 2019).

Acknowledgements The authors would like to thank Prof. Dr. Peter Grathwohl and Prof. Dr. Todd Ehlers, from the University of Tübingen, for the help during the development of this research. We would also like to thank Dr. Lorenzo Marchi and an anonymous reviewer for their comments, which contributed to significantly improve the manuscript.

Author contributions Mr. VCC worked on the development and writing of the manuscript and organized and collected fieldwork data. Dr. FAGVR organized the fieldwork campaign and contributed to the development and organization of the manuscript. Dr. FMD'A aided the development and writing of the manuscript. Dr. AL contributed to the writing and organization of the manuscript. Dr. CVSC aided the collection of fieldwork data and data processing. Mr. VV helped in the collection of fieldwork data and data processing. Mr. MFG contributed to the organization of the fieldwork and data collection. Mr. ATO contributed to fieldwork data collection and organization of the manuscript. Ms. AFL aided the development of the manuscript and the acquisition of rain gauge data. Dr. FV contributed to satellite meteorological data. Dr. AJPF contributed to the meteorological data and development of the manuscript. Dr. CCS organized and aided the acquisition of high-resolution aerial photographs. Dr. ESSL aided the acquisition of high-resolution aerial photographs and the organization of the fieldwork campaign. Ms. LMRR aided the organization of the fieldwork campaign. Dr. Giordano aided the organization of the fieldwork campaign. Dr. CZ worked on the writing and organization of the manuscript.

Funding Open Access funding enabled and organized by Projekt DEAL. This study was financed in part by the Coordenação de Aperfeiçoamento de Pessoal de Nível Superior—Brasil (CAPES)—Finance Code 001. Dr. Pereira Filho was sponsored by Conselho Nacional de Desenvolvimento Científico e Tecnológico—Brasil (CNPq) under Grant 302349/2017-6.

Data availability The datasets generated during our study are available from the corresponding author upon request.

Declarations

Conflict of interest The authors declare that they do not have any competing interests.

References

Agência Nacional de Águas—ANA (2020) Rain gauges "Garuva - 420580301A" and "Estrada Geral Quiriri - 420580302A". Available at http://www.snirh.gov.br/hidroweb/serieshistoricas

Amponsah W, Marchi L, Zoccatelli D, Boni G, Cavalli M, Comiti F, Crema S, Lucía A, Marra F, Borga M (2016) Hydrometeorological characterization of a flash flood associated with major geomorphic effects: assessment of peak discharge uncertainties and analysis of the runoff response. J Hydrometeorol 17(12):3063–3077

Arcement GJ, Schneider VR (1989) Guide for selecting manning's roughness coefficients for natural channels and flood plains. U. S. Geological Survey Water-Supply Paper 2339

Back AJ, Henn JA, Oliveira JLR (2011) Heavy rainfall equations for Santa Catarina, Brazil. Rev Bras Ci Solo 35:2127–2134

Beguería S, Van Asch T, Malet J, Gröndahl S (2009) A GIS-based numerical model for simulating the kinematics of mud and debris flows over complex terrain. Nat Hazard Earth Sys 9(6):1897–1909

Beniston M (2009) Trends in joint quantiles of temperature and precipitation in Europe since 1901 and projected for 2100. Geophys Res Lett 36:L07707

Bennett G, Molnar P, McArdell B, Schlunegger F, Burlando P (2013) Patterns and controls of sediment production, transfer and yield in the Illgraben. Geomorphology 188:68–82
Berger C, McArdell BW, Schlunegger F (2011) Direct measurement of channel erosion by debris flows, Illgraben. Switzerland J Geophys Res 116:F01002
Bianco G, Franzi L (2000) Estimation of debris-flow volumes from storm events. In: Wieczorek GF, Naeser ND (eds) Debris-flow hazards mitigation: mechanics, prediction and assessment. Balkema, Rotterdam, pp 441–448
Borga M, Stoffel M, Marchi L, Marra F, Jakob M (2014) Hydrogeomorphic response to extreme rainfall in headwater systems: Flash floods and debris flows. J Hydrol 518:194–205
Centro Nacional de Monitoramento e Alerta de Desastres Naturais—Cemaden (2020) Rain gauges "Garuva - 420580301A" and "Estrada Geral Quiriri - 420580302A". Available at http://www.cemaden.gov.br/mapainterativo/
Chang C, Lin P, Tsai C (2011) Estimation of sediment volume of debris flow caused by extreme rainfall in Taiwan. Eng Geol 123(1–2):83–90
Chen NS, Yue ZQ, Cui P (2007) A rational method for estimating maximum discharge of a landslide-induced debris flow: a case study from south western China. Geomorphology 84:44–58
Destro E, Amponsah W, Nikolopoulos E, Marchi L, Marra F, Zoccatelli D, Borga M (2018) Coupled prediction of flash flood response and debris flow occurrence: application on an alpine extreme flood event. J Hydrol 558:225–237
de Haas T, Densmore AL (2019) Debris-flow volume quantile prediction from catchment morphometry. Geology 47:791–794
Gabet E, Sternberg P (2008) The effects of vegetative ash on infiltration capacity, sediment transport, and the generation of progressively bulked debris flows. Geomorphology 101(4):666–673
Gaume E, Borga M (2008) Post-flood field investigations in upland catchments after major flash floods: proposal of a methodology and illustrations. J Flood Risk Manag 1(4):175–189
George DL, Iverson RM (2011) A two-phase debris-flow model that includes coupled evolution of volume fractions, granular dilatancy, and pore-fluid pressure. Ital J Eng Geol Environ 43:415–424
Giorgi F, Im ES, Coppola E, Diffenbaugh NS, Gao XJ, Mariotti L, Shi Y (2011) Higher hydroclimatic intensity with global warming. J Climate 24:5309–5324
Gramani MF, Martins VTS (2016) Debris flows occurrence by intense rains on January 13, 2014 at Itaoca City, São Paulo, Brazil: impacts and field observations. Int Symposium Landslides, Napoli, Italy, p 8
Gregoretti C, Degetto M, Bernard M, Boreggio M (2018) The debris flow occurred at Ru Secco Creek, Venetian Dolomites, on 4 august 2015: analysis of the phenomenon, its characteristics and reproduction by models. Front Earth Sci 6:80
Huggel C, Clague JJ, Korup O (2012) Is climate change responsible for changing landslide activity in high mountains? Earth Surf Proc Landf 37:77–91
Hungr O, Morgan GC, Kellerhals R (1984) Quantitative analysis of debris torrent hazards for design of remedial measures. Can Geotech J 21:663–677
Hungr O, Leroueil S, Picarelli L (2014) The Varnes classification of landslide types, an update. Landslides 11(2):167–194
Iverson R (2000) Landslide triggering by rain infiltration. Water Resour Res 36(7):1897–1910
Iverson RM, Reid ME, Logan M, LaHusen RG, Godt JW, Griswold JP (2011) Positive feedback and momentum growth during debris-flow entrainment of wet bed sediment. Nat Geosci 4:116–121
Jakob M (2005a) Debris-flow hazard analysis. In: Jakob M, Hungr O (eds) Debris-flow hazards and related phenomena. Springer-Verlag, Berlin, pp 411–443
Jakob M (2005b) A size classification for debris flows. Eng Geol 79:151–161
Kanji MA, Cruz PT, Massad F, Araujo FHA (1997) Basic and common characteristics of debris flows. Proc 2nd Pan Am Symposium Rio De Janeiro 10:223–231
Kanji MA, Cruz PT, Massad F (2007) Debris flow affecting the Cubatão oil refinery. Brazil Landslides 5(1):71–82
Kean JW, McCoy SW, Tucker GE, Staley DM, Coe JA (2013) Runoff-generated debris flows: observations and modeling of surge initiation, magnitude, and frequency. J Geophys Res Earth Surf 118:2190–2207
Kobiyama M, Michel G, Engster E, Paixão M (2015) Historical analyses of debris flow disaster occurrences and of their scientific investigation in Brazil. Labor e Engenho 9(4):76
Kronfellner-Kraus G (1985) Quantitative estimation of torrent erosion. Int Symposium Erosion Debris Flow Dis Prev, Tsukuba, Japan, pp 107–110
Lacerda W (2007) Landslide initiation in saprolite and colluvium in southern Brazil: field and laboratory observations. Geomorphology 87(3):104–119
Lang A, Moya J, Corominas J, Schrott L, Dikau R (1999) Classic and new dating methods for assessing the temporal occurrence of mass movements. Geomorphology 30(1–2):33–52

Liu KF, Li HC, Hsu YC (2009) Debris flow hazard assessment with numerical simulation. Nat Hazards 49:137–161
Lucía A, Comiti F, Borga M, Cavalli M, Marchi L (2015) Dynamics of large wood during a flash flood in two mountain catchments. Nat Hazards Earth Syst Sci 15:1741–1755
Lucía A, Schwientek M, Eberle J, Zarfl C (2018) Planform changes and large wood dynamics in two torrents during a severe flash flood in Braunsbach, Germany 2016. Sci Total Environ 640–641:315–326
Luna B, Remaître A, van Asch T, Malet J, van Westen C (2012) Analysis of debris flow behavior with a one-dimensional run-out model incorporating entrainment. Eng Geol 128:63–75
Maack R (2002) Geografia física do Estado do Paraná. Curitiba, Imprensa Oficial, p 440
Marchi L, D'Agostino V (2004) Estimation of debris-flow magnitude in the Eastern Italian Alps. Earth Surf Process Landf 29(2):207–220
Marchi L, Cavalli M, Sangati M, Borga M (2009) Hydrometeorological controls and erosive response of an extreme alpine debris flow. Hydrol Process 23(19):2714–2727
Marchi L, Brunetti M, Cavalli M, Crema S (2019) Debris-flow volumes in northeastern Italy: relationship with drainage area and size probability. Earth Surf Process Landf 44(4):933–943
Marengo J, Camarinha P, Alves L, Diniz F, Betts R (2021) Extreme rainfall and hydro-geo-meteorological disaster risk in 1.5, 2.0, and 4.0°C global warming scenarios: an analysis for brazil. Front Clim 3
Massad F (2002) Corridas de massas geradas por escorregamentos de terra: relação entre a área deslizada e a intensidade de chuva. In: XII Congresso Brasileiro de Mecânica dos Solos e Engenharia Geotécnica. São Paulo, São Paulo
Milne F (2008) Topographic and material controls on the Scottish debris flow geohazard. University of Dundee, Thesis
Mocochinski AY, Scheer MB (2014) Campos de altitude na serra do mar paranaense: aspectos florísticos. Floresta 38(4):625–640
Pánek T (2014) Recent progress in landslide dating. Progr Phys Geogr Earth Environ 39(2):168–198
Pak J, Lee J (2008) A Statistical sediment yield prediction model incorporating the effect of fires and subsequent storm events. J Am Water Resour as 44(3):689–699
Pereira Filho AJ, Vemado F, Reis FAGV, Giordano LC, Cerri RI, Santos CC, Lopes ESS, Gramani MF, Ogura AT, Zaine JE, Cerri LES, Augusto Filho O, D'Affonseca FM, Amaral CS (2018) A Step towards integrating CMORPH precipitation estimation with rain gauge measurements. Adv in Meteorol 2018:1–24
Petley D (2012) Global patterns of loss of life from landslides. Geology 40:927–930
Reid ME, Coe JA, Dianne LB (2016) Forecasting inundation from debris flows that grows volumetrically during travel, with application to the Oregon Coast Range, USA. Geomorphology 273:396–411
Rickenmann D (1999) Empirical relationships for debris flows. Nat Hazards 19(1):47–77
Rickenmann D, Zimmermann M (1993) The 1987 debris flows in Switzerland: documentation and analysis. Geomorphology 8:175–189
Rickenmann D, Koschni A (2010) Sediment loads due to fluvial transport and debris flows during the 2005 flood events in Switzerland. Hydrol Process 24(8):993–1007
Rickenmann D (2016) Methods for the quantitative assessment of channel processes in torrents (steep streams). CRC Press, Taylor and Francis Group, Leiden
Rosi A, Canavesi V, Segoni S, Dias Nery T, Catani F, Casagli N (2019) Landslides in the mountain region of Rio de Janeiro: a proposal for the semi-automated definition of multiple rainfall thresholds. Geosciences 9:203
Santi PM, Dewolfe VG, Higgins JD, Cannon SH, Gartner JE (2008) Sources of debris flow material in burned areas. Geomorphology 96(3–4):310–321
Santi P (2014) Precision and accuracy in debris-flow volume measurement. Environ Eng Geosci 20(4):349–359
Shen P, Zhang L, Wong H, Peng D, Zhou S, Zhang S, Chen C (2020) Debris flow enlargement from entrainment: a case study for comparison of three entrainment models. Eng Geol 270:105581
Steeb N, Rickenmann D, Badoux A, Rickli C, ScheWaldner P (2017) Large wood recruitment processes and transported volumes in Swiss mountain streams during the extreme flood of August 2005. Geomorphology 279:112–127
Stoffel M (2010) Magnitude–frequency relationships of debris flows: a case study based on field surveys and tree-ring records. Geomorphology 116:67–76
Stoffel M, Huggel C (2012) Effects of climate change on mass movements in mountain environments. Prog Phys Geogr 36:421–439

Surian N, Righini M, Lucía A, Nardi L, Amponsah W, Benvenuti M, Borga M, Cavalli M, Comiti F, Marchi L, Rinaldi M, Viero A (2016) Channel response to extreme floods: insights on controlling factors from six mountain rivers in northern Apennines, Italy. Geomorphology 272:78–91

Tabarelli M, Pinto L, Silva J, Hirota M, Bedê L (2005) Challenges and opportunities for biodiversity conservation in the Brazilian Atlantic forest. Conserv Biol 19(3):695–700

Takahashi T (1991) Debris Flow. A.A. Balkema, Rotterdam

Takahashi T, Nakagawa H, Harada T, Yamashiki Y (1992) Routing Debris flows with particle segregation. J Hydraul Eng 118:1490–1507

Takahashi T (2006) Debris flows: mechanics prediction and countermeasures. Taylor and Francis, Balkema

Takei A (1984) Interdependence of sediment budget between individual torrents and a river-system. Proc Int Symp INTERPRAEVENT, Villach, Austria 2:35–48

Tang C, Rengers N, van Asch T, Yang Y, Wang G (2011) Triggering conditions and depositional characteristics of a disastrous debris flow event in Zhouqu city, Gansu Province, northwestern China. Nat Hazards Earth Syst Sci 11(11):2903–2912

Teixeira MS, Satyamurty P (2011) Trends in the frequency of intense precipitation events in southern and southeastern Brazil during 1960–2004. J Climate 24:1913–1921

Varnes DJ (1978) Slope movement types and processes. In: Schuster RL, Krizek RJ (Eds) Special report 176: landslides: analysis and control. Transportation and Road Research Board, National Academy of Science, Washington DC, pp 11–33

Vieira B, Gramani M (2015) Serra do Mar: The Most "Tormented" Relief in Brazil. In: Migon P (ed) World Geomorphological landscapes. Springer, Berlin, pp 285–297

Westra S, Fowler H, Evans J, Alexander L, Berg P, Johnson F, Kendon E, Lenderink G, Roberts N (2014) Future changes to the intensity and frequency of short-duration extreme rainfall. Rev Geophys 52:522–555

Wilford DJ, Sakals ME, Innes JL, Sidle RC, Bergerud WA (2004) Recognition of debris flow, debris flood and flood hazard through watershed morphometrics. Landslides 1(1):61–66

Winter MG, Shearer B (2014) Landslide hazard and risk in a changing climate. In: Sassa K, Canuti P, Yin Y (eds) Landslide Science for a Safer Geoenvironment: The International Programme on Landslides (IPL), vol 1. Springer, New York, pp 281–286

Wolle CM, Hachich W (1989) Rain-induced landslides in Southeastern Brazil. Proc 12th Int Conf Soil Mech Found Eng Rio De Janeiro, Brazil 3:1639–1642

Authors and Affiliations

Victor Carvalho Cabral[1,2] · Fábio Augusto Gomes Vieira Reis[1] · Fernando Mazo D'Affonseca[2] · Ana Lucía[2] · Claudia Vanessa dos Santos Corrêa[1] · Vinicius Veloso[1] · Marcelo Fischer Gramani[3] · Agostinho Tadashi Ogura[3] · Andrea Fregolente Lazaretti[4] · Felipe Vemado[5] · Augusto José Pereira Filho[5] · Claudia Cristina dos Santos[6] · Eymar Silva Sampaio Lopes[6] · Lis Maria Reoni Rabaco[7] · Lucilia do Carmo Giordano[1] · Christiane Zarfl[2]

[1] Applied Geology Department, Earth and Exact Sciences Institute, São Paulo State University – UNESP, Av. 24A, 1555, Rio Claro, São Paulo, Brazil

[2] Geo- und Umweltforschungszentrum (GUZ), University of Tübingen, Schnarrenbergstraße 94-96, Tübingen, Germany

[3] Institute for Technological Research – IPT, Av. Prof. Almeida Prado, 532, São Paulo, São Paulo, Brazil

[4] Brazilian Geological Service – CPRM, Rua Costa, 55, São Paulo, São Paulo, Brazil

[5] Institute of Astronomy, Geophysics and Atmospheric Sciences, University of São Paulo – USP, Rua do Matão, 1226, São Paulo, São Paulo, Brazil

[6] National Institute for Space Research – INPE, Av. dos Astronautas, 1758, São José dos Campos, São Paulo, Brazil

[7] Centro de Pesquisas e Desenvolvimento – CENPES, Av. Horácio de Macedo, 950, Rio de Janeiro, Rio de Janeiro, Brazil